

Shortcuts in a Nonlinear Dynamical Braneworld in Six Dimensions

Bertha Cuadros-Melgar *

Instituto de Física, Universidade de São Paulo
C.P.66.318, CEP 05315-970, São Paulo, Brazil

Abstract

We consider a dynamical brane world in a six-dimensional space-time containing a singularity. Using the Israel conditions we study the motion of a 4-brane embedded in this setup. We analyse the brane behaviour when its position is perturbed about a fixed point and solve the full nonlinear dynamics in the several possible scenarios. We also investigate the possible gravitational shortcuts and calculate the delay between graviton and photon signals and the ratio of the corresponding subtended horizons.

PACS numbers: 04.50.+h 11.27.+d 97.60.Lf 98.80.-k

*e-mail: bertha@fma.if.usp.br

1 Introduction

It has recently been argued that there might exist some extra spatial dimensions, not in the traditional Kaluza-Klein (KK) scheme [1] where extra dimensions are compactified on a radius of the order of Planck scale, but in a scenario where they could be large. Certainly, the extra dimensions idea is not completely new but it is also related to string theories. Among the existing models the ten-dimensional $E_8 \times E_8$ heterotic string theory seems to be the most acceptable candidate to describe our world. This theory is related to an 11-dimensional spacetime, where the 11th dimension is compactified via a Z_2 orbifold symmetry. In this setup the standard model particles are confined to a four-dimensional spacetime, while the gravitons propagate in full spacetime.

Large extra dimensions were also recalled to solve the hierarchy problem [2]. However, it was the work of Randall and Sundrum [3, 4] which suscitated a renewed interest on these grounds. In this model our world is identified with a domain wall in five-dimensional anti de Sitter (AdS) spacetime. In their first paper, Randall and Sundrum proposed a mechanism to solve the hierarchy problem by a small extra dimension, while in their second paper, the braneworld with a positive tension was investigated.

In this paper we consider a six-dimensional model where the bulk contains a singularity and is bounded by a four-dimensional brane containing matter. This brane is a thick brane with the usual three infinite spatial directions and an additional coordinate compactified in a small radius that can be of Planck size like in the KK models [1] or even of submillimetric size as in the Arkani-Hamed, Dimopoulos and Dvali (ADD) models [2], which makes it unavailable to the brane observers. In this way, this “effective” picture corresponds to our universe. The static case has been already studied in [6] where AdS-Schwarzschild and AdS-Reissner-Nordström embeddings were considered. The case of domain walls moving in bulks containing non-charged singularities has also been studied in [7, 8]. Brane models in AdS space with Schwarzschild singularities have been used to understand the AdS/CFT correspondence and look like promising theoretical models [9].

The motivation for a six-dimensional model comes from the fact that spacetimes with more than one extra dimension can allow for solutions with more appealing features, particularly in spacetimes where the curvature of the internal space is non-zero. More extra dimensions also relax the fine-tunings

of the fundamental parameters. On the other hand, the ADD model [2], which relates the Planck mass to the fundamental mass in $(4+n)$ dimensions through the size of the transverse dimensions, foresees the existence of $n \geq 2$ extra dimensions. The possibility $n = 1$ remains excluded from experimental bounds since there are no observed violations of the Newton's law at distances of the order of the solar system.

According to the model, photons are confined to the brane and gravitons can propagate in all five spatial directions, then there is a possibility that gravitational fields while propagating out of the brane speed up due to the warped bulk geometry reaching farther distances in smaller time than light propagating inside the brane, a scenario that for a resident of the brane (as ourselves) implies shortcuts [5, 6, 10, 11, 12].

The existence of shortcuts implies that causality is violated from the point of view of a four-dimensional observer; however, it is perfectly defined through N -dimensional geodesics for an observer in the bulk. Thus, two points apparently causally disconnected in four dimensions could be causally connected by gravitational shortcuts. This fact accounts for a possible solution of the horizon problem. As it was pointed out in [13], if high redshifts were available, shortcuts appearing before nucleosynthesis are serious mediators of homogenization of the matter on the brane and then they could provide an explanation alternative to inflation to this problem. Other alternative approaches have also considered a varying speed of light [14]. Moreover, if inflation took part on the brane, the causal structure is definitely changed by shortcuts possibly leading to a non-usual period of causal evolution of scales, what could be responsible for distinct predictions in the cosmic microwave background structure for inflationary models.

The paper is organized as follows. In section 2 we describe the six-dimensional model considered along this work, derive the equation system governing the brane motion from the point of view of a bulk observer and write the geodesic equation corresponding to the shortest graviton path in the bulk as well as the expression for the delay between graviton and photon flight times. Section 3 is devoted to studying the brane behaviour when its position is perturbed about a fixed point. In section 4 we provide the solutions of geodesic equation and brane equation of motion in the different scenarios resulting from the combination of the parameters appearing in the model and show the existence of several shortcuts. We also find the time delay and the ratio between the horizons subtended by gravitons and photons.

Finally, we discuss our results in section 5.

2 The Brane Cosmological Model

We consider a six-dimensional model described by the following metric

$$ds^2 = -n^2(t, y, z)dt^2 + a^2(t, y, z)d\Sigma_k^2 + b^2(t, y, z)dy^2 + c^2(t, y, z)dz^2, \quad (1)$$

where $d\Sigma_k^2$ represents the metric of the three-dimensional spatial sections with $k = -1, 0, 1$ corresponding to a hyperbolic, a flat and an elliptic space, respectively.

The matter content on the brane is directly related to the jump of the extrinsic curvature tensor across the brane [8, 15]. This relation has been derived in the case of a static brane in a previous work [6]. Here we generalize our result for the Israel conditions to include the case of a brane moving with respect to the coordinate system. Its position at any bulk time t will be denoted by

$$z = \mathcal{R}(t). \quad (2)$$

The extrinsic curvature tensor on the brane is given by

$$K_{MN} = \eta_M^L \nabla_L \tilde{n}_N, \quad (3)$$

where \tilde{n}^A is a unit vector field normal to the brane worldsheet and

$$\eta_{MN} = g_{MN} - \tilde{n}_M \tilde{n}_N \quad (4)$$

is the induced metric on the brane.

In order to compute the components of \tilde{n}^A , we use the relations

$$g_{MN} \tilde{n}^M \tilde{n}^N = 1 \quad , \quad g_{MN} \tilde{n}^M u^N = 0, \quad (5)$$

where we have introduced the unit velocity vector corresponding to the brane, which reads

$$u^A = \left\{ \frac{dt}{d\tau}, 0, 0, 0, 0, \frac{dz}{d\tau} \right\}. \quad (6)$$

The relation between dt (the bulk time) and $d\tau$ (the brane time) can be found from the induced metric,

$$\begin{aligned} ds_{induced}^2 &= - \left[n^2(t, \mathcal{R}(t)) - c^2(t, \mathcal{R}(t)) \dot{z}^2 \right] dt^2 + a^2(t, \mathcal{R}(t)) d\Sigma_{(4)}^2 \\ &= -d\tau^2 + a^2(\tau) d\Sigma_{(4)}^2, \end{aligned} \quad (7)$$

where a dot means derivative with respect to the bulk time t . We obtain

$$d\tau = n(t, \mathcal{R}(t)) \sqrt{1 - \frac{c^2(t, \mathcal{R}(t))}{n^2(t, \mathcal{R}(t))} \dot{\mathcal{R}}^2} dt \equiv n\gamma^{-1} dt. \quad (8)$$

Thus, (6) can be written as

$$u^A = \frac{\gamma}{n} \{1, 0, 0, 0, 0, \dot{\mathcal{R}}\}, \quad (9)$$

and from (5) we can easily obtain

$$\tilde{n}^A = \left\{ \frac{c \dot{\mathcal{R}}}{n^2 \sqrt{1 - \frac{c^2}{n^2} \dot{\mathcal{R}}^2}}, 0, 0, 0, 0, \frac{1}{c \sqrt{1 - \frac{c^2}{n^2} \dot{\mathcal{R}}^2}} \right\}. \quad (10)$$

Now we can calculate the components of the extrinsic curvature tensor by substituting (10) into (3). The non-zero components are

$$\begin{aligned} K_0^0 &= \frac{c}{n^2} \left(1 - \frac{c^2(t, \mathcal{R}(t))}{n^2(t, \mathcal{R}(t))} \right)^{-5/2} \times \\ &\times \left\{ \ddot{\mathcal{R}} + \frac{nn'}{c^2} - \dot{\mathcal{R}} \left(\frac{\dot{n}}{n} - 2 \frac{\dot{c}}{c} \right) - \dot{\mathcal{R}}^2 \left(2 \frac{n'}{n} - \frac{c'}{c} \right) - \dot{\mathcal{R}}^3 \frac{c\dot{c}}{n^2} \right\}, \end{aligned} \quad (11)$$

$$K_6^6 = \dot{\mathcal{R}} K_0^0, \quad K_6^0 = -\frac{c^2}{n^2} \dot{\mathcal{R}} K_0^0, \quad (12)$$

$$K_i^j = \frac{1}{c} \left(1 - \frac{c^2(t, \mathcal{R}(t))}{n^2(t, \mathcal{R}(t))} \right)^{-1/2} \left\{ \frac{a'}{a} + \frac{\dot{a}}{a} \frac{c^2}{n^2} \dot{\mathcal{R}} \right\} \delta_i^j, \quad (13)$$

$$K_5^5 = \frac{1}{c} \left(1 - \frac{c^2(t, \mathcal{R}(t))}{n^2(t, \mathcal{R}(t))} \right)^{-1/2} \left\{ \frac{b'}{b} + \frac{\dot{b}}{b} \frac{c^2}{n^2} \dot{\mathcal{R}} \right\}, \quad (14)$$

$$K_6^6 = -\frac{c^2}{n^2} \dot{\mathcal{R}}^2 K_0^0, \quad (15)$$

where all the coefficients take values on the brane.

2.1 The Israel Conditions

The energy-momentum tensor on the brane located at z_0 can be written as

$$T_{MN}^{(b)} = \frac{\delta(z - z_0)}{c} \{(\rho + p)u_M u_N + p\eta_{MN}\}. \quad (16)$$

We also define a tensor \hat{T}_{AB} as

$$\hat{T}_{AB} \equiv T_{AB} - \frac{1}{4}T\eta_{AB}. \quad (17)$$

The Israel junction conditions [16] are given by

$$[K_{\mu\nu}] = -\kappa_{(6)}^2 \hat{T}_{\mu\nu}, \quad (18)$$

where the brackets stand for the jump across the brane and $K_{\mu\nu} = e_\mu^A e_\nu^B K_{AB}$, where e_μ^A form a basis of the vector space tangent to the brane worldvolume.

The non-zero components of (17) are given by

$$\hat{T}_0^0 = -\frac{\gamma^2}{c} \left\{ \frac{3\rho + 4p}{4} \right\}, \quad (19)$$

$$\hat{T}_0^6 = \dot{\mathcal{R}}\hat{T}_0^0, \quad \hat{T}_6^0 = -\frac{c^2}{n^2}\dot{\mathcal{R}}\hat{T}_0^0, \quad (20)$$

$$\hat{T}_i^j = \frac{\rho}{4c}\delta_i^j, \quad \hat{T}_5^5 = \hat{T}_i^i, \quad (21)$$

$$\hat{T}_6^6 = -\frac{c^2}{n^2}\dot{\mathcal{R}}^2\hat{T}_0^0. \quad (22)$$

The left-hand side of (18) can be calculated taking into account the mirror symmetry across the brane

$$[K_{\mu\nu}] = K_{\mu\nu}(t, \mathcal{R}(t)^+) - K_{\mu\nu}(t, \mathcal{R}(t)^-) = -2K_{\mu\nu}(t, \mathcal{R}(t)). \quad (23)$$

At this point it is convenient to choose a specific bulk metric of the form (1) satisfying six-dimensional Einstein equations. This is given by

$$ds^2 = -h(z)dt^2 + a^2(z)d\Sigma_k^2 + h^{-1}(z)dz^2, \quad (24)$$

where

$$a(z) = \frac{z}{l}, \quad (25)$$

$$d\Sigma_k^2 = \frac{dr^2}{1 - kr^2} + r^2 d\Omega_{(2)}^2 + (1 - kr^2)dy^2, \quad (26)$$

and

$$h(z) = k + \frac{z^2}{l^2} - \frac{M}{z^3} + \frac{Q^2}{z^6} \quad (27)$$

with $l^{-2} \propto -\Lambda$ (Λ being the cosmological constant, which can be positive or negative) and M and Q^2 are constants.

We should stress that dy can be written as $dy = R_c d\varphi$, with φ an angle with the usual periodicity 2π . Thus, the coordinate y is compactified under some mechanism such that its radius of compactification R_c is small enough to evade experimental detection [1, 2]. This makes the local observers have the picture of living on an effective three-dimensional brane.

Metric (24) contains a singularity located at $z = 0$. It is valid on the $z < \mathcal{R}(t)$ parts of surfaces of constant t and its reflection, by the Z_2 orbifold symmetry, is valid on the $z > \mathcal{R}(t)$ parts. If $M = 0$ and $Q^2 = 0$, then (24) is simply the metric of de Sitter or anti de Sitter spacetime according to the sign of l^2 .

With this Ansatz the Israel conditions (18) reduce to only two equations, which read as

$$\ddot{\mathcal{R}} + \frac{1}{2} \frac{h'}{h^3} \dot{\mathcal{R}}^4 - 3 \frac{h'}{h} \dot{\mathcal{R}}^2 + \frac{1}{2} h h' = -\kappa_{(6)}^2 \left(\frac{3\rho + 4p}{8} \right) h^2 \left(1 - \frac{\dot{\mathcal{R}}^2}{h^2} \right)^{3/2} \quad (28)$$

$$\frac{a'}{a} + \frac{\dot{\mathcal{R}}}{h^2} \frac{\dot{a}}{a} = \kappa_{(6)}^2 \frac{\rho}{8} \left(1 - \frac{\dot{\mathcal{R}}^2}{h^2} \right)^{1/2},$$

where again all the metric coefficients must be evaluated on the brane. System (28) describes the full nonlinear dynamics of the brane embedded in the static bulk (24).

2.2 The Geodesic Equation and the Time Delay

We consider two points on the brane r_A and r_B . In general there are more than one null geodesic connecting these points in the $1 + 5$ spacetime. The trajectories of photons must be on the brane and those of gravitons may be outside. The graviton path is defined equating (24) to zero. Since we are looking for a path that minimizes t when the final point r_B is on the brane, the problem reduces to an Euler-Lagrange problem [5]. Then as in [17] the shortest graviton path is given by

$$\ddot{\mathcal{R}}_g + \left(\frac{1}{\mathcal{R}_g} - \frac{3}{2} \frac{h'}{h} \right) \dot{\mathcal{R}}_g^2 + \frac{1}{2} h h' - \frac{h^2}{\mathcal{R}_g} = 0. \quad (29)$$

We can also calculate the time delay between the photon travelling on the brane and the gravitons travelling in the bulk. Since both signals cover the same distance [13],

$$\int_0^{\tau_f + \Delta\tau} \frac{d\tau_\gamma}{\mathcal{R}(\tau_\gamma)} = \int_0^{t_f} \frac{dt_g}{\mathcal{R}_g(t_g)} \sqrt{h(\mathcal{R}_g) - \frac{\dot{\mathcal{R}}_g(t)^2}{h(\mathcal{R}_g)}}, \quad (30)$$

the difference between photon and graviton flight times measured by an observer on the brane can approximately be written in terms of the bulk time t as [17]

$$\Delta\tau \simeq \mathcal{R}(t_f) \int_0^{t_f} dt \left(\frac{1}{\mathcal{R}_g(t)} \sqrt{h(\mathcal{R}_g) - \frac{\dot{\mathcal{R}}_g(t)^2}{h(\mathcal{R}_g)}} - \frac{1}{\mathcal{R}(t)} \frac{d\tau}{dt} \right). \quad (31)$$

It is also interesting to look at the ratio between the horizons subtended by the photons travelling on the brane and the gravitons travelling in the bulk. This ratio uses the same quantities previously quoted for the time delay,

$$\frac{g}{\gamma} = \frac{\int_0^{t_f} \frac{dt}{\mathcal{R}_g(t)} \sqrt{h(\mathcal{R}_g) - \frac{\dot{\mathcal{R}}_g(t)^2}{h(\mathcal{R}_g)}}}{\int_0^{t_f} \frac{dt}{\mathcal{R}(t)} \frac{d\tau}{dt}}. \quad (32)$$

3 Brane Fluctuations

In this section we study perturbatively the brane behaviour at a fixed point. We define the background solution as the case where the brane position is frozen, *i.e.*

$$z = \mathcal{R}(t) = \bar{\mathcal{R}} = \text{const.} \quad (33)$$

Then the system (28) reduces to

$$\frac{1}{2} \frac{h'}{h} = -\frac{\kappa_{(6)}^2}{8} (3\bar{\rho} + 4\bar{p}) \quad (34)$$

$$\frac{a'}{a} = \frac{\kappa_{(6)}^2}{8} \bar{\rho}. \quad (35)$$

The equations of motion for the brane fluctuations can be obtained linearizing the exact equations of motion (28) about the “equilibrium” configuration. They read as

$$\begin{aligned}\frac{\delta\ddot{\mathcal{R}}}{h^2} + \frac{1}{2}\delta\left(\frac{h'}{h}\right) &= -\frac{\kappa_{(6)}^2}{8}(3\delta\rho + 4\delta p) \\ \delta\left(\frac{a'}{a}\right) &= \frac{\kappa_{(6)}^2}{8}\delta\rho.\end{aligned}\tag{36}$$

From the explicit expressions of h (with $Q = 0$) and a we can find

$$\delta\left(\frac{a'}{a}\right) = -\frac{\kappa_{(6)}^4}{64}\bar{\rho}^2\delta\mathcal{R} \equiv m_a^2\delta\mathcal{R}\tag{37}$$

$$\frac{1}{2}\delta\left(\frac{h'}{h}\right) = \left\{-\frac{\kappa_{(6)}^4}{32}(3\bar{\rho} + 4\bar{p})^2 + \frac{\frac{1}{l^2} - 6\frac{M}{\mathcal{R}^5}}{k + \frac{\mathcal{R}^2}{l^2} - \frac{M}{\mathcal{R}^3}}\right\}\delta\mathcal{R} \equiv m_h^2\delta\mathcal{R}.\tag{38}$$

As we can see from (36), the brane fluctuations are bound to the matter fluctuations. However, when we have the case of adiabatic matter fluctuations

$$\delta p = v_s^2\delta\rho,\tag{39}$$

we can derive an equation for the brane fluctuations with an appropriate linear combination of (36)

$$\frac{\delta\ddot{\mathcal{R}}}{h^2} + \left(m_h^2 + (3 + 4v_s^2)m_a^2\right)\delta\mathcal{R} = 0,\tag{40}$$

while the matter fluctuations will be related to the brane ones by

$$\frac{\kappa_{(6)}^2}{8}\delta\rho = m_a^2\delta\mathcal{R}.\tag{41}$$

Assuming an equation of state $p = \omega\rho$, (40) finally reads

$$\frac{\delta\ddot{\mathcal{R}}}{h^2} + \left\{\frac{\frac{1}{l^2} - 6\frac{M}{\mathcal{R}^5}}{k + \frac{\mathcal{R}^2}{l^2} - \frac{M}{\mathcal{R}^3}} - (7 + 8\omega)(3 + 4\omega)\frac{\kappa_{(6)}^4}{64}\bar{\rho}^2\right\}\delta\mathcal{R} = 0.\tag{42}$$

The constant M can be expressed in terms of $\bar{\mathcal{R}}$ and ω from the Israel conditions for a static brane [6] as

$$M = \frac{2\bar{\mathcal{R}}^3}{8\omega + 3} \left\{ (4\omega + 3)k + 4(\omega + 1)\frac{\bar{\mathcal{R}}^2}{l^2} \right\}. \quad (43)$$

In the case of a flat domain wall ($k = 0$, $\omega = -1$), the term inside braces in (42) can be interpreted as an effective cosmological constant on the brane,

$$\frac{1}{\bar{\mathcal{R}}^2} - \frac{\kappa_{(6)}^4}{64}\bar{\rho}^2 \equiv -\Lambda_{eff}, \quad (44)$$

which vanishes when we take into account (35). This corresponds to the Randall-Sundrum condition [3, 4] in six dimensions. Then, the effective cosmological constant on the brane is zero.

Therefore, we are left with the equation of motion for a free scalar field as in five dimensions [15, 18]. In this case the brane is at rest and the equilibrium position $\bar{\mathcal{R}}$ can be chosen arbitrarily. However, a small departure from this position results in a runaway behaviour.

This result is compatible with the numerical solution of the full nonlinear system (28) as we will see in the next section.

4 Nonlinear Brane Dynamics

The system (28) describing the brane dynamics can be numerically solved for several combinations of M , Q^2 , k and l^2 . When M , Q^2 and k vanish, the solution for $\mathcal{R}(t)$ is a constant or a linear function in t depending on the given initial condition for $\dot{\mathcal{R}}$, and we verify the behaviour found through brane fluctuations.

For M and Q^2 non-zero we have solved (28) in the typical cases of a domain wall ($\omega = -1$), matter ($\omega = 0$) and radiation ($\omega = 1/3$) dominated branes. In figure 1 we show all the possibilities for the bulk metric according to the form that $h(z)$ takes due to M , Q^2 , k and l^2 combinations, which we study in this section. Some of our results are also illustrated in what follows together with the solution of the geodesic equation (29) in order to verify the possibility of having shortcuts. We have also calculated the time delays and the ratio between graviton and photon horizons for the examples

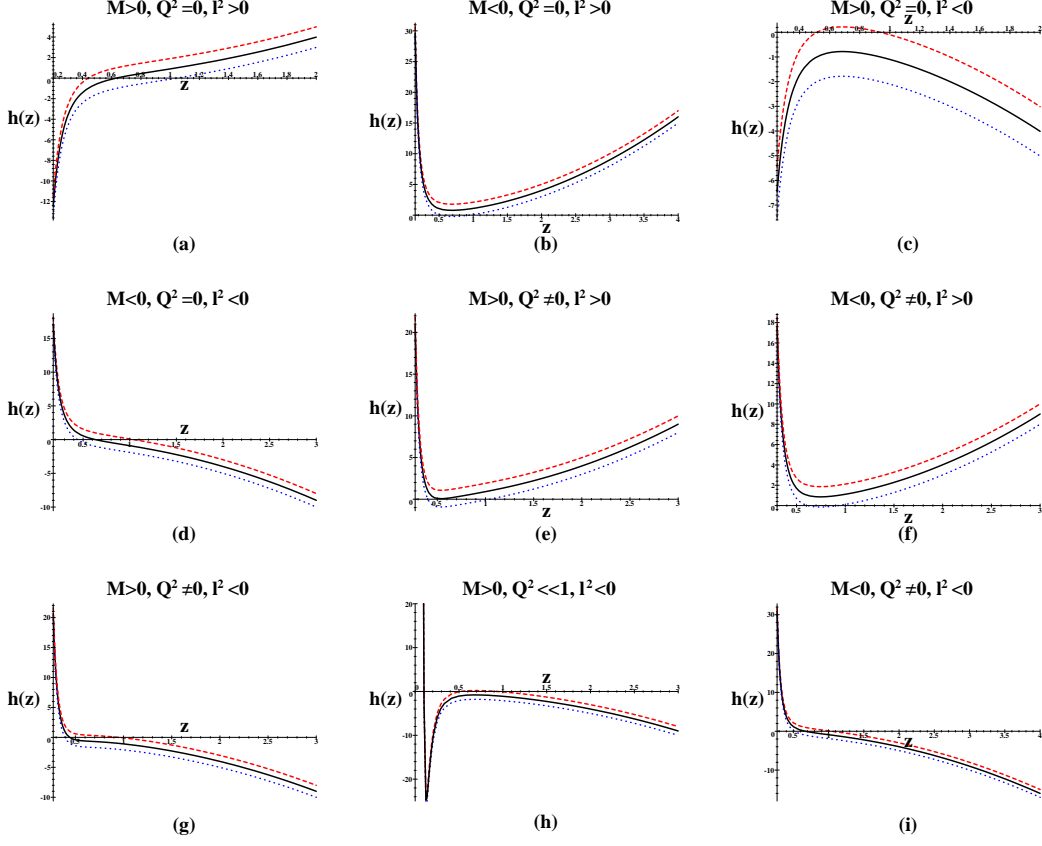


Figure 1: $h(z)$ for all the possible combinations of M , Q^2 and l^2 , including $k = 1$ (dashed lines), $k = 0$ (solid lines) and $k = -1$ (dotted lines) cases.

of shortcuts appearing in this paper, these are shown in Table 3 together with the graviton bulk flight time and its corresponding brane time according to the equation (8).

We have classified all cases according to the sign of the M parameter and to whether we are in dS or AdS bulks. Moreover, we studied the zero charge black hole as well as the Reissner-Nordström-type solutions, namely eight

cases.

M	k	l^2	Bulk	DW	MDB	RDB	Geodesic
+	1	+	AdS-Schwarzschild	$\rightarrow r_H/G$	$\rightarrow r_H$	$\rightarrow r_H$	$\rightarrow r_H^*/G$
+	0,-1	+	AdS-top. black hole	$\rightarrow r_H$	$\rightarrow r_H$	$\rightarrow r_H$	$\rightarrow r_H^*$
-	0,1	+	AdS-naked singularity	G	$\rightarrow 0$	$\rightarrow 0$	$G^*/\rightarrow 0$
-	-1	+	AdS-top. black hole	$\rightarrow r_H$	$\rightarrow r_H$	$\rightarrow r_H$	$\rightarrow r_H$
+	1	-	dS-Schwarzschild	$\rightarrow r_H/r_c$	$\rightarrow r_H/r_c$	$\rightarrow r_H/r_c$	$\rightarrow r_H/r_c^{*\dagger}$
+	0,-1	-	dS-cosm. singularity	no solution	no solution	no solution	no solution
-	0, ± 1	-	dS-naked singularity	$\rightarrow r_c$	$\rightarrow 0/r_c$	$\rightarrow 0/r_c$	$\rightarrow 0/r_c^{*\dagger}$

Table 1: Scale factor and geodesics evolution (uncharged case). The arrow indicates the behaviour tendency, which depends on the initial conditions. G means growing behaviour. The $*$ or the \dagger in the last column indicates the possibility of shortcuts for the matter and radiation-dominated branes or the domain wall, respectively.

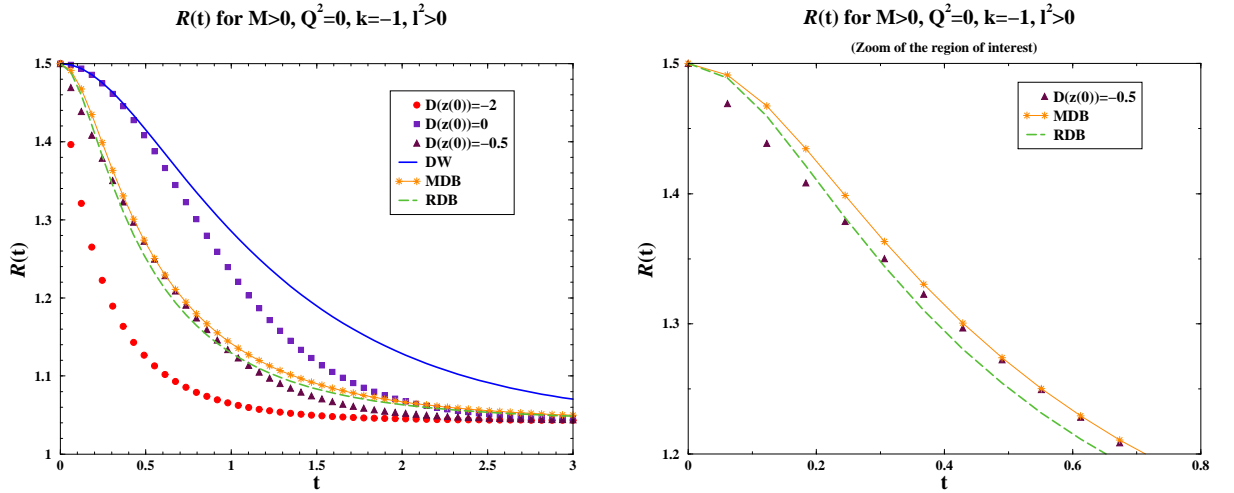


Figure 2: Scale factor evolution for domain wall, matter and radiation-dominated branes and geodesics when $M > 0$, $Q^2 = 0$ and $l^2 > 0$.

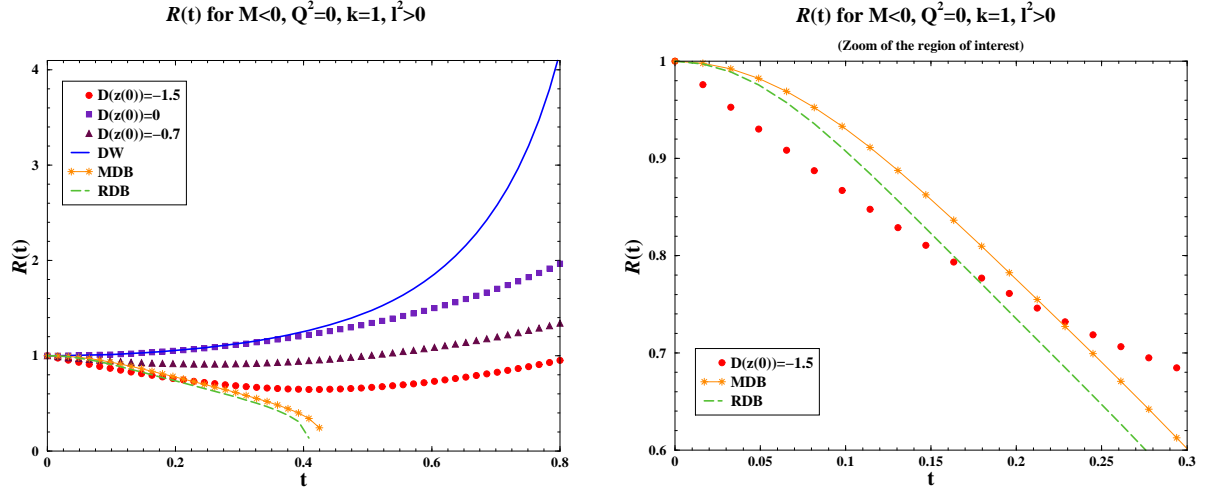


Figure 3: Scale factor evolution for domain wall, matter and radiation-dominated branes and geodesics when $M < 0$, $Q^2 = 0$ and $l^2 > 0$.

First, let us consider the zero charge case. The following results have also been summarized in table 1 for a better comprehension of the several solutions.

4.1 $M > 0$, $Q^2 = 0$, $l^2 > 0$

For positive both M and l^2 when $k = 1$, the bulk is anti de Sitter-Schwarzschild solution, while for $k \neq 1$ we have a “topological” black hole with a flat or hyperbolic event horizon in an asymptotically anti de Sitter space. This case is shown in figure 1(a).

For a domain wall ($\omega = -1$) and $k = 1$ the brane falls into the event horizon r_H when the initial condition for the brane position is near r_H , otherwise $\mathcal{R}(t)$ grows. On the other hand, for $k \neq 1$ the brane always falls into r_H .

In the case of a matter-dominated brane ($\omega = 0$) the brane falls into the event horizon for any k . This behaviour is also verified for a radiation-dominated brane ($\omega = 1/3$).

Let us see now the geodesic behaviour. When $k = 1$ and the initial

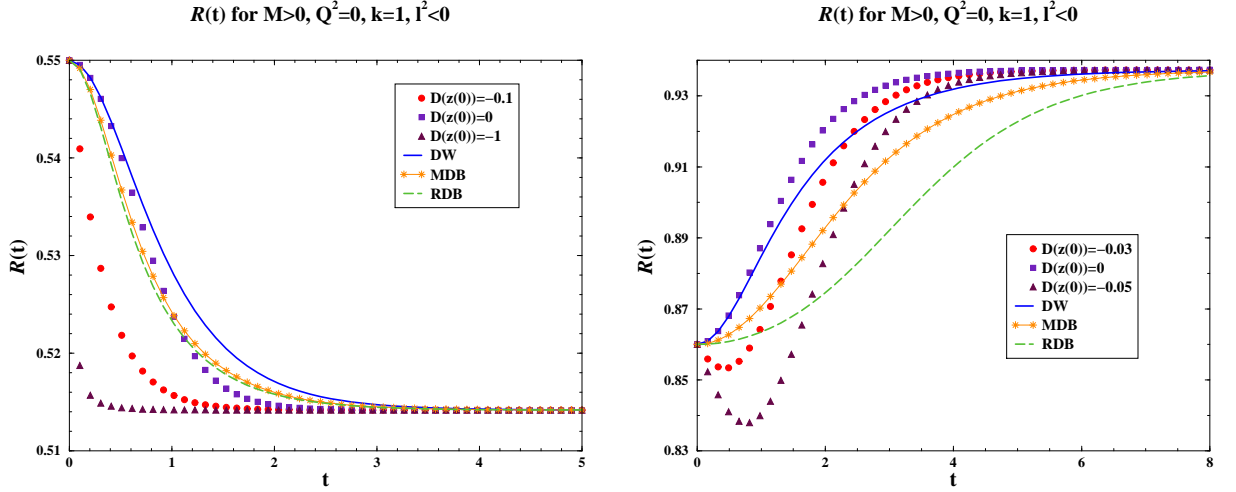


Figure 4: Scale factor evolution for domain wall, matter and radiation-dominated branes and geodesics when $M > 0$, $Q^2 = 0$ and $l^2 < 0$.

condition on the brane is chosen near r_H , the geodesics fall into the event horizon. Some of them follow the domain wall at the beginning and others leave the matter or radiation-dominated branes returning after a short time (shortcut geodesics) and leaving again the branes to fall into the singularity. Conversely, if the initial condition is taken far from the event horizon, the geodesics grow accompanying the domain wall initially, though their growth is slower; however, they never return to it after their decoupling. When $k \neq 1$, independently of the initial condition the geodesics behave in the same way as the previous case when the initial condition is taken near r_H and we again find some shortcuts for the matter and radiation-dominated branes before all the geodesics fall into the event horizon. Some results are shown in figure 2.

4.2 $M < 0$, $Q^2 = 0$, $l^2 > 0$

As we can see from figure 1(b), for negative M and positive l^2 when $k = -1$, h describes a topological black hole in an asymptotically anti de Sitter space

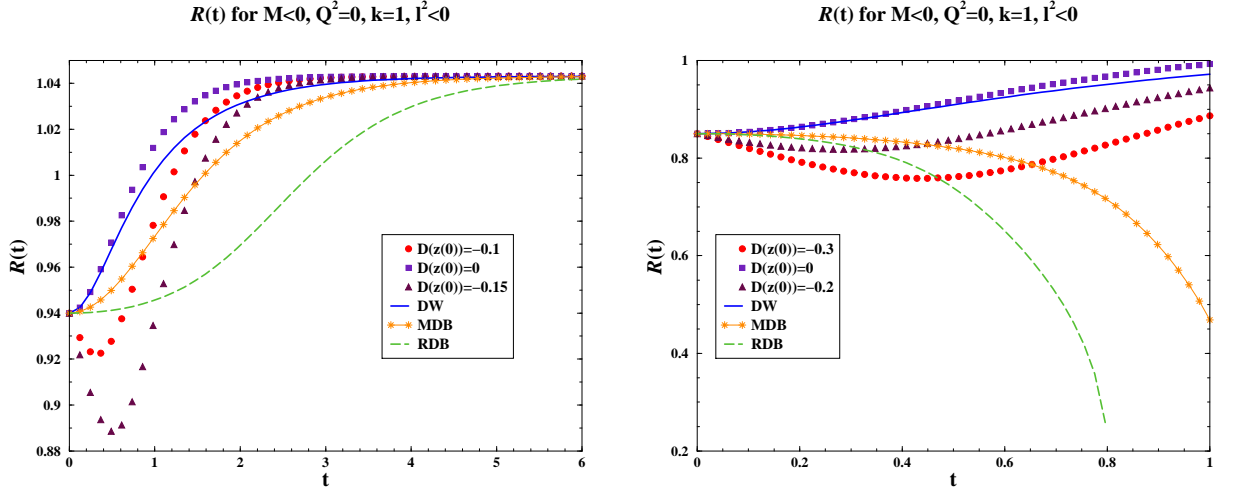


Figure 5: Scale factor evolution for domain wall, matter and radiation-dominated branes and geodesics when $M < 0$, $Q^2 = 0$ and $l^2 < 0$.

with hyperbolic event horizon. If $k \neq -1$, there is a timelike naked singularity and the metric is asymptotically anti de Sitter.

The solutions of the brane equation of motion (28) display the following features. In the case of a domain wall, when $k = -1$, the brane falls into the event horizon; while if $k \neq -1$, the solution for $\mathcal{R}(t)$ grows.

For $(\omega = 0)$ the matter-dominated brane falls into the naked singularity when $k \neq -1$ and into the event horizon if $k = -1$. The radiation-dominated brane displays the same behaviour.

On the other hand, the solutions of equation (29) show that when $k \neq -1$, the geodesics grow slower than the domain wall. Some of them are shortcuts for matter or radiation-dominated branes since they leave and return to them before the branes reach the naked singularity. Furthermore, if the geodesic (negative) initial velocity is big enough, it can fall into the naked singularity. Besides, when $k = -1$, all the geodesics fall into the event horizon. We can see some results in figure 3.

M	Q^2	k	l^2	Bulk	DW	MDB	RDB	Geodesic
+	+	0	+	AdS-naked singularity	$\rightarrow \infty/B$	$B/\rightarrow 0$	$B/\rightarrow 0$	$B^{*\dagger}/\rightarrow \infty^\dagger/0$
+	+	1	+	AdS-naked singularity	$\rightarrow \infty$	$\rightarrow 0$	$\rightarrow 0$	G^*
+	+	-1	+	AdS-Top.ch. black hole	$\rightarrow r_H$	$\rightarrow r_H$	$\rightarrow r_H$	$\rightarrow r_H$
+	\ll	0,-1	+	AdS-Top.ch. black hole	$\rightarrow r_H$	$\rightarrow r_H$	$\rightarrow r_H$	$\rightarrow r_H^*$
+	\ll	1	+	AdS-Reissner-Nordström	$\rightarrow r_H/\infty$	$\rightarrow r_H$	$\rightarrow r_H$	$\rightarrow r_H^*$
-	+	0,1	+	AdS-naked singularity	$\rightarrow \infty$	$\rightarrow 0$	$\rightarrow 0$	G^*
-	+	-1	+	AdS-Top.ch. black hole	$\rightarrow r_H$	$\rightarrow r_H$	$\rightarrow r_H$	$\rightarrow r_H^*$
+	+	0,-1	-	dS-naked singularity	$\rightarrow r_c$	$\rightarrow r_c$	$\rightarrow 0/r_c$	$\rightarrow r_c^{*\dagger}$
+	+	1	-	dS-naked singularity	$\rightarrow r_c$	$B/\rightarrow 0/r_c$	$\rightarrow 0/r_c$	$\rightarrow r_c^{*\dagger}$
+	\ll	0,-1	-	dS-naked singularity	$\rightarrow r_c$	$\rightarrow r_c$	$\rightarrow 0/r_c$	$\rightarrow r_c^{*\dagger}/0$
+	\ll	1	-	dS-Reissner-Nordström	$\rightarrow r_H/r_c$	$\rightarrow r_H/r_c$	$\rightarrow r_H/r_c$	$\rightarrow r_H^*/r_c^{*\dagger}$
-	+	0, \pm 1	-	dS-naked singularity	$\rightarrow r_c$	$\rightarrow 0/r_c$	$\rightarrow 0/r_c$	$\rightarrow r_c^{*\dagger}/0$

Table 2: Scale factor and geodesics evolution (charged case). B and G mean bouncing and growing behaviour, respectively. The $*$ or the \dagger in the last column indicates the possibility of shortcuts for the matter and radiation-dominated branes or the domain wall, respectively.

4.3 $M > 0$, $Q^2 = 0$, $l^2 < 0$

In the case of positive M , negative l^2 and $k = 1$, the metric is de Sitter-Schwarzschild with event and cosmological horizons given by the zeros of $h(\mathcal{R})$. If $k \neq 1$, there is a cosmological singularity at $\mathcal{R} = 0$ in the asymptotically de Sitter background. See figure 1(c).

In the case of a domain wall for $k = 1$, the solutions for $\mathcal{R}(t)$ converge either to the event or the cosmological horizon. For $k \neq 1$, there is no solution since \mathcal{R} turns to be a time coordinate. The same behaviour is observed for matter and radiation-dominated branes.

Since the solutions to the brane equation of motion just appear when $k = 1$, the solutions of the geodesic equation only have physical meaning in this case. In this way we found that the geodesics reach either the event or the cosmological horizon. In the latter case there are many shortcuts for the matter or radiation-dominated branes as well as for the domain wall before all of them reach the cosmological horizon. Some results are illustrated in figure 4.

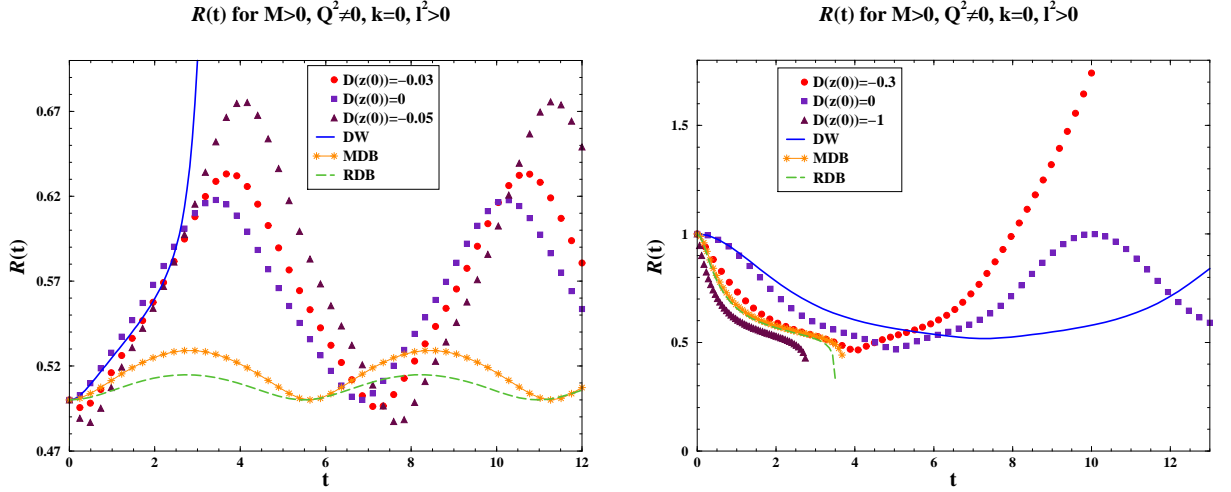


Figure 6: Scale factor evolution for domain wall, matter and radiation-dominated branes and geodesics when $M > 0$, $Q^2 \neq 0$ and $l^2 > 0$.

4.4 $M < 0$, $Q^2 = 0$, $l^2 < 0$

When M and l^2 are both negative, the bulk metric displays a timelike naked singularity in asymptotically de Sitter space. There is also a cosmological horizon which geometry is determined by k as we can see from figure 1(d).

In the case of a domain wall for any k the solution $\mathcal{R}(t)$ converges to the cosmological horizon.

When $(\omega = 0)$, the matter-dominated brane either falls into the naked singularity or converges to the cosmological horizon independently of the value of k . This same result was found for a radiation-dominated brane.

On the other hand, the geodesics either fall into the naked singularity when the initial velocity is negative enough or converge to the cosmological horizon for any k . In the latter case we found several shortcuts for the domain wall and the branes. We can see some results in figure 5.

Now let us consider the charged solutions. As in the uncharged case, we also show a summary of our results in table 2.

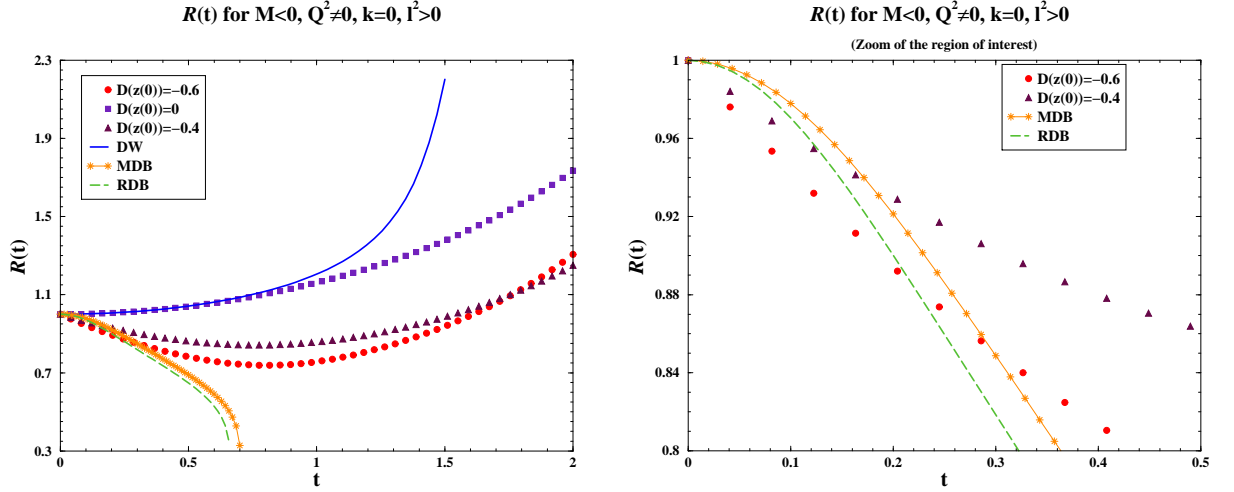


Figure 7: Scale factor evolution for domain wall, matter and radiation-dominated branes and geodesics when $M < 0$, $Q^2 \neq 0$ and $l^2 > 0$.

4.5 $M > 0$, $Q^2 \neq 0$, $l^2 > 0$

When M and l^2 are both positive, for $k = -1$ the metric describes a topological charged black hole in asymptotically anti de Sitter space with hyperbolic horizon. While for $k \neq -1$, there is a timelike naked singularity and the bulk is asymptotically anti de Sitter (see figure 1(e)). Note that if the charge is small, all the metrics describe topological charged black holes in anti de Sitter bulks. In particular, when $k = 1$, we have anti de Sitter-Reissner-Nordström bulk.

Let us see the solutions of the brane equation of motion. In the case of a domain wall there are different behaviours for each value of k . When $k = 0$, $\mathcal{R}(t)$ bounces for the initial condition $\mathcal{R}(0)$ greater than or equal to the minimum of $h(\mathcal{R})$; otherwise, it diverges to infinity. When $k = 1$, $\mathcal{R}(t)$ diverges to infinity. When $k = -1$, the domain wall falls into the event horizon. For small charges $\mathcal{R}(t)$ converges to the event horizon except when $k = 1$, where it can also grow or diverge to infinity after a certain initial value. In the limit $Q \rightarrow 0$ we also verified that our solutions converge to

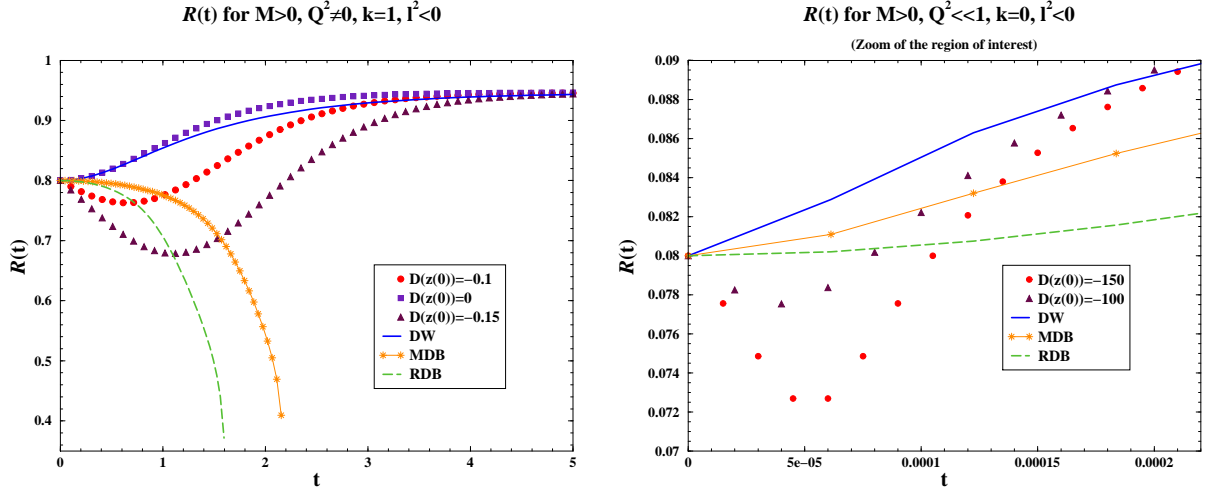


Figure 8: Scale factor evolution for domain wall, matter and radiation-dominated branes and geodesics when $M > 0$, $Q^2 \neq 0$ and $l^2 < 0$.

those in section 4.1.

For a matter-dominated brane ($\omega = 0$) we again found different behaviours for each k . When $k = 0$, $\mathcal{R}(t)$ bounces for the initial condition $\mathcal{R}(0)$ less than or equal to the minimum of $h(\mathcal{R})$; otherwise, it falls into the naked singularity. When $k = 1$, $\mathcal{R}(t)$ goes to the naked singularity. When $k = -1$, it falls into the event horizon. For small charges the brane always falls into the event horizon. Again when $Q \rightarrow 0$ we recover the solutions in section 4.1.

In the case of a radiation-dominated brane ($\omega = 1/3$) the behaviour of the solution is somewhat similar to the matter-dominated brane case. When $k = 0$, $\mathcal{R}(t)$ bounces for the initial condition $\mathcal{R}(0)$ less than or equal to the minimum of $h(\mathcal{R})$, but it falls into the naked singularity when the initial condition is near 0 or when it is greater than the minimum of $h(\mathcal{R})$. When $k = 1$, $\mathcal{R}(t)$ goes to the naked singularity. When $k = -1$, it falls into the event horizon as the previous case. For small charges we have the same behaviour as in the matter-dominated brane case.

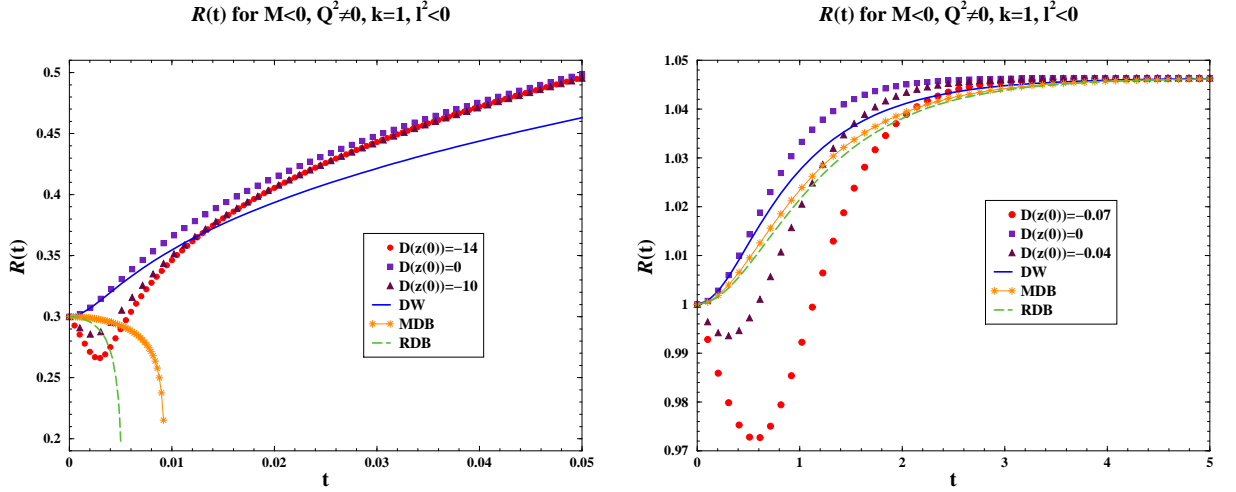


Figure 9: Scale factor evolution for domain wall, matter and radiation-dominated branes and geodesics when $M < 0$, $Q^2 \neq 0$ and $l^2 < 0$.

Now let us investigate the geodesic behaviour. When $k = 0$, the geodesics bounce for the initial condition less than or equal to the minimum of $h(\mathcal{R})$ in the same way as matter or radiation-dominated branes producing several shortcuts in all brane cases. However, when the initial condition is greater than the minimum of $h(\mathcal{R})$, the geodesics can continue to bounce or escape after one oscillation or even fall into the naked singularity as a result of increasing the initial (negative) velocity; in this case we just found shortcuts for the domain wall as long as the geodesics complete at least one oscillation. For small charges an event horizon is formed and the geodesics fall into it but there are still some small shortcuts for matter or radiation-dominated branes. When $k = 1$, the geodesics grow slower than the domain wall producing shortcuts just for matter or radiation-dominated branes. For small charges the geodesics either diverge or fall into the event horizon. When $k = -1$, all the geodesics fall into the event horizon as the branes and there are no shortcuts. For small charges the geodesics fall into the event horizon but can yield some shortcuts in the very beginning of their paths for radiation

	DW				MDB				RDB			
Fig.	t	τ	$\Delta\tau$	g/γ	t	τ	$\Delta\tau$	g/γ	t	τ	$\Delta\tau$	g/γ
2	-	-	-	-	.54	.408	.004	1.011	.27	.238	.002	1.009
3	-	-	-	-	.23	.25	.01	1.047	.18	.191	.005	1.033
4	2.39	.563	.009	1.015	1.27	.393	.003	1.007	.95	.306	.002	1.006
4	3.51	.76	.03	1.035	2.33	.67	.02	1.024	1.74	.56	.01	1.019
5	1.58	.53	.02	1.028	.89	.412	.007	1.017	.66	.326	.004	1.013
5	2.20	.69	.04	1.061	1.45	.63	.03	1.046	1.06	.54	.02	1.039
5	-	-	-	-	.66	.47	.03	1.064	.47	.32	.01	1.046
5	-	-	-	-	.44	.300	.006	1.021	.33	.224	.003	1.015
6	2.03	.464	.006	1.013	.80	.232	.002	1.008	.64	.192	.001	1.007
6	-	-	-	-	1.11	.318	.007	1.022	.94	.283	.006	1.020
6	5.5	1.6	.2	1.206	-	-	-	-	-	-	-	-
6	6.2	2.5	.1	1.074	-	-	-	-	-	-	-	-
7	-	-	-	-	.30	.259	.006	1.024	.22	.191	.003	1.018
7	-	-	-	-	.175	.169	.002	1.011	.13	.126	.001	1.008
8	3.07	.91	.06	1.065	1.01	.47	.01	1.026	.73	.337	.006	1.019
8	-	-	-	-	1.56	.76	.07	1.094	1.1	.51	.03	1.061
8	2.2E-4	2E-3	2E-4	1.084	1.4E-4	1.7E-3	1E-4	1.072	1.1E-4	1.6E-3	1E-4	1.069
8	1.9E-4	1.8E-3	7E-5	1.035	1.1E-4	1.4E-3	3E-5	1.024	8.2E-5	1.1E-3	2E-5	1.022
9	.013	.036	.004	1.106	.0052	.023	.002	1.077	.004	.019	.001	1.062
9	.012	.035	.002	1.056	.0042	.0186	5E-3	1.030	.0031	.0139	3E-3	1.023
9	2.4	.52	.02	1.029	2.2	.52	.01	1.027	2.0	.51	.01	1.026
9	1.5	.355	.004	1.010	1.3	.339	.003	1.008	1.1	.314	.002	1.007

Table 3: Bulk time t , brane time τ , time delays $\Delta\tau$ and ratio between graviton and photon horizons g/γ for shortcut geodesics.

or matter-dominated branes. Some of these cases appear in figure 6.

4.6 $M < 0$, $Q^2 \neq 0$, $l^2 > 0$

For negative M , positive l^2 and $k = -1$, the metric describes a topological charged black hole in asymptotically anti de Sitter spacetime with hyperbolic horizon. While for $k \neq -1$ there is a timelike naked singularity and the bulk is asymptotically anti de Sitter as is shown in figure 1(f).

In the case of $\omega = -1$ and for $k = -1$ the domain wall falls into the event horizon. If in turn $k \neq -1$, the solution $\mathcal{R}(t)$ diverges to infinity.

When we consider a matter-dominated brane for $k = -1$, the brane behaves in the same way as a domain wall; however, if $k \neq -1$, it falls into the naked singularity. This same behaviour is observed for a radiation-dominated brane.

As for the solutions to the geodesic equation, when $k = -1$, the geodesics fall into the event horizon and some of them can produce shortcuts for radiation or matter-dominated branes before their falling. If $k \neq -1$, the geodesics grow and yield shortcuts for matter or radiation-dominated branes. Some results are shown in figure 7.

4.7 $M > 0$, $Q^2 \neq 0$, $l^2 < 0$

In the case of positive M and negative l^2 the metric describes a timelike naked singularity in asymptotically de Sitter space with a cosmological horizon as we see in figure 1(g). However, for a small charge the $k = 1$ metric turns out to be de Sitter-Reissner-Nordström with Cauchy, event and cosmological horizons as it is shown in figure 1(h).

For a domain wall the solution $\mathcal{R}(t)$ converges to the cosmological horizon for any k . For a small charge this behaviour also applies except for $k = 1$, when the domain wall can also fall into the event horizon.

The case of a matter-dominated brane displays an interesting behaviour. When $k = 1$, $\mathcal{R}(t)$ bounces when the initial condition $\mathcal{R}(0)$ is less than or equal to the only saddle point in $h(\mathcal{R})$; otherwise, it falls into the naked singularity or converges to the cosmological horizon if the initial condition $\mathcal{R}(0)$ is very near it. When $k \neq 1$, the solutions converge to the cosmological horizon. For a small charge the solutions converge to the cosmological horizon and also to the event horizon in the case $k = 1$.

When we consider a radiation-dominated brane, we see that it either falls into the naked singularity or converges to the cosmological horizon for any k . For a small charge the solutions behave in the same way except if $k = 1$ when the brane converges either to the cosmological or the event horizon.

Let us see the geodesic behaviour. For any k all the geodesics converge to the cosmological horizon and produce several shortcuts for all brane cases. When the charge is very small, an event horizon appears in the case $k = 1$ and the geodesics can either converge to the cosmological or the event hori-

zons. The geodesics converging to the cosmological horizon produce shortcuts for all brane cases, while the geodesics falling into the event horizon yield shortcuts just for matter or radiation-dominated branes. On the other hand, when $k \neq 1$, the geodesics converge to the cosmological horizon after producing some shortcuts for all brane cases, unless their initial (negative) velocity reaches a threshold after which they fall into the naked singularity. Some results are illustrated in figure 8.

4.8 $M < 0$, $Q^2 \neq 0$, $l^2 < 0$

When M and l^2 are both negative, the metric describes a timelike naked singularity in asymptotically de Sitter space for any k (see figure 1(i)).

As for the solutions of the brane equation of motion, in the case of a domain wall all the solutions converge to the cosmological horizon.

When we consider a matter-dominated brane, $\mathcal{R}(t)$ either falls into the naked singularity or converges to the cosmological horizon for any k . The same behaviour applies for a radiation-dominated brane.

As for the geodesics, they converge to the cosmological horizon and produce several shortcuts for all brane cases for any k . However, when the initial condition is taken near the singularity and the initial velocity is negative enough, the geodesics can reach the singularity and no shortcut appears. We can see some results in figure 9.

5 Discussion and Conclusions

In the present work we have studied the behaviour of a brane embedded in a six-dimensional de Sitter or anti de Sitter spacetime containing a singularity covered by at least one horizon in the case of black hole type solutions or a timelike naked singularity. The system of equations describing this behaviour from the point of view of an observer in the bulk appears to be highly nonlinear. Before numerically solving this system we have considered fluctuations about a fixed brane position in order to have a better insight of the whole problem. We have concluded that the case of a flat domain wall with vanishing effective cosmological constant reproduces the equation of motion for a free scalar field as in five dimensions [15, 18]. The “equilibrium” position can be chosen arbitrarily but there is no stability.

By solving the full nonlinear system we found different behaviours for the several scenarios appearing due to all the combinations of M , Q^2 , k and l^2 taken into account. We chose some typical values for ω , i.e. domain wall, matter and radiation-dominated branes, in order to illustrate the solutions. The results show branes getting away from the singularity, falling into it, converging to cosmological horizons when they exist or even bouncing between a minimum and maximum values.

The bouncing behaviour found in some of our solutions of the brane equation of motion appears to be in good agreement with the recent investigations in five dimensions [19], where universes bouncing from a contracting to an expanding phase without encountering past and/or future singularities appear. In this way these results could provide support for a singularity-free cosmology or to the so-called cyclic universe scenarios [20].

Finally, we also studied the geodesic behaviour in every scenario found in the present work. Contrarily to the case of a static brane, where shortcuts appeared under very restrictive conditions [6], the present model of a dynamic brane embedded in a static bulk displays shortcuts in almost all cases and under very mild conditions. Moreover, despite the fact that the time delay between graviton and photon flight time is not percentually so big as in other models [17] (what is also evident from the ratio between graviton and photon horizons), it exists and can eventually be measured by the brane observer, although further considerations are certainly needed in a stricter realistic model. On the other hand, the fact that shortcuts are abundant in the studied setups lends further support to the idea of solving the horizon problem via thermalization by graviton exchange [17, 13]; however, we should stress that this is not a proof of the solution of the problem yet.

Acknowledgements: I would like to thank Elcio Abdalla for useful discussions and for reading the manuscript. This work has been supported by Fundação de Amparo à Pesquisa do Estado de São Paulo (**FAPESP**), Brazil.

References

- [1] T. Kaluza, *Sitzungsberichte Preussische Akademie der Wissenschaften* **K1** (1921) 966; O. Klein, *Z. F. Physik* **37** (1926) 895; O. Klein, *Nature*

118 (1926) 516.

- [2] N. Arkani-Hamed, S. Dimopoulos and G. Dvali, *Phys. Lett.* **B429** (1998) 263. I. Antoniadis, N. Arkani-Hamed, S. Dimopoulos and G. Dvali, *Phys. Lett.* **B436** (1998) 257.
- [3] L. Randall and R. Sundrum, *Phys. Rev. Lett.* **83** (1999) 3370.
- [4] L. Randall and R. Sundrum, *Phys. Rev. Lett.* **83** (1999) 4690.
- [5] E. Abdalla, B. Cuadros-Melgar, S. Feng and B. Wang, *Phys. Rev.* **D65** (2002) 083512; [hep-th/0109024].
- [6] E. Abdalla, A. Casali, B. Cuadros-Melgar, *Nucl. Phys.* **B644** (2002) 201; [hep-th/0205203].
- [7] P. Kraus, *J. High Energy Phys.* **9912** (1999) 011; [hep-th/9910149].
- [8] H.A. Chamblin and H.S. Reall, *Nucl.Phys.* **B562** (1999) 133; [hep-th/9903225].
- [9] Bin Wang, Elcio Abdalla and Ru Keng Su, *Phys. Lett.* **B503** (2001) 394, *Mod. Phys. Lett.* **A17** (2002) 23.
- [10] C. Csáki, J. Erlich and C. Grojean, *Nucl.Phys.* **B604** (2001) 312; [hep-th/0012143].
- [11] H. Ishihara, *Phys. Rev. Lett.* **86** (2001) 381. R. Caldwell and D. Langlois, *Phys. Lett.* **B511** (2001) 129; [gr-qc/0103070].
- [12] D. J. Chung and K. Freese, *Phys. Rev.* **D61** (2000) 023511; [hep-ph/9906542]. *Phys. Rev.* **D62** (2000) 063513; [hep-ph/9910235].
- [13] E. Abdalla and A. G. Casali, [hep-th/0208008].
- [14] See J. Magueijo, *Rept. Prog. Phys.* **66** (2003) 2025; [astro-ph/0305457] for a review on VSL theories.
- [15] P. Binétruy, C. Deffayet, D. Langlois, *Nucl.Phys.* **B615** (2001) 219; [hep-th/0101234].
- [16] W. Israel, *Nuovo Cimento* **B44** (1966) 1.

- [17] E. Abdalla and B. Cuadros-Melgar, *Phys. Rev.* **D67** (2003) 084012; [hep-th/0209101].
- [18] C. Charmousis, R. Gregory, V. A. Rubakov, *Phys. Rev.* **D62** (2000) 067505; [hep-th/9912160].
- [19] S. Mukherji and M. Peloso, *Phys. Lett.* **B547** (2002) 297; [hep-th/0205180]. A. J. Mevdev, [hep-th/0205251]. P. Kanti and K. Tamvakis, *Phys. Rev.* **D68** (2003) 024014; [hep-th/0303073].
- [20] P.J. Steinhardt and N. Turok, *Science* **296** (2002) 1436; [astro-ph/0204479].